Supplement of Atmos. Meas. Tech., 17, 1599–1615, 2024
https://doi.org/10.5194/amt-17-1599-2024-supplement

Atmospheric Measurement Techniques
Open Access

Supplement of

First validation of high-resolution satellite-derived methane emissions from an active gas leak in the UK

Emily Dowd et al.

Correspondence to: Emily Dowd (eeed@leeds.ac.uk)

Supplemental Information

Section S1. Gas leak site

Figure S1. Image of gas leak site works taken on 12th June 2023.

Figure S2. Image of dead vegetation (circled in red) at gas leak site taken on 12th June 2023.

Figure S3. © Google Earth 2023 image of the gas leak site taken in June 2023, showing works being done on the west site of the railway line.

Section S2. Leak Location

Table S1. Location of the gas leak estimated from the satellite observations

Date	Latitude (°N)	Longitude (°W)
27/03/2023	51.95097	2.09956
20/04/2023	51.95098	2.09956
20/05/2023	51.95086	2.09961
22/05/2023	51.95027	2.10012
26/05/2023	51.95079	2.09967

Section S3. Flux Estimation Flow Charts

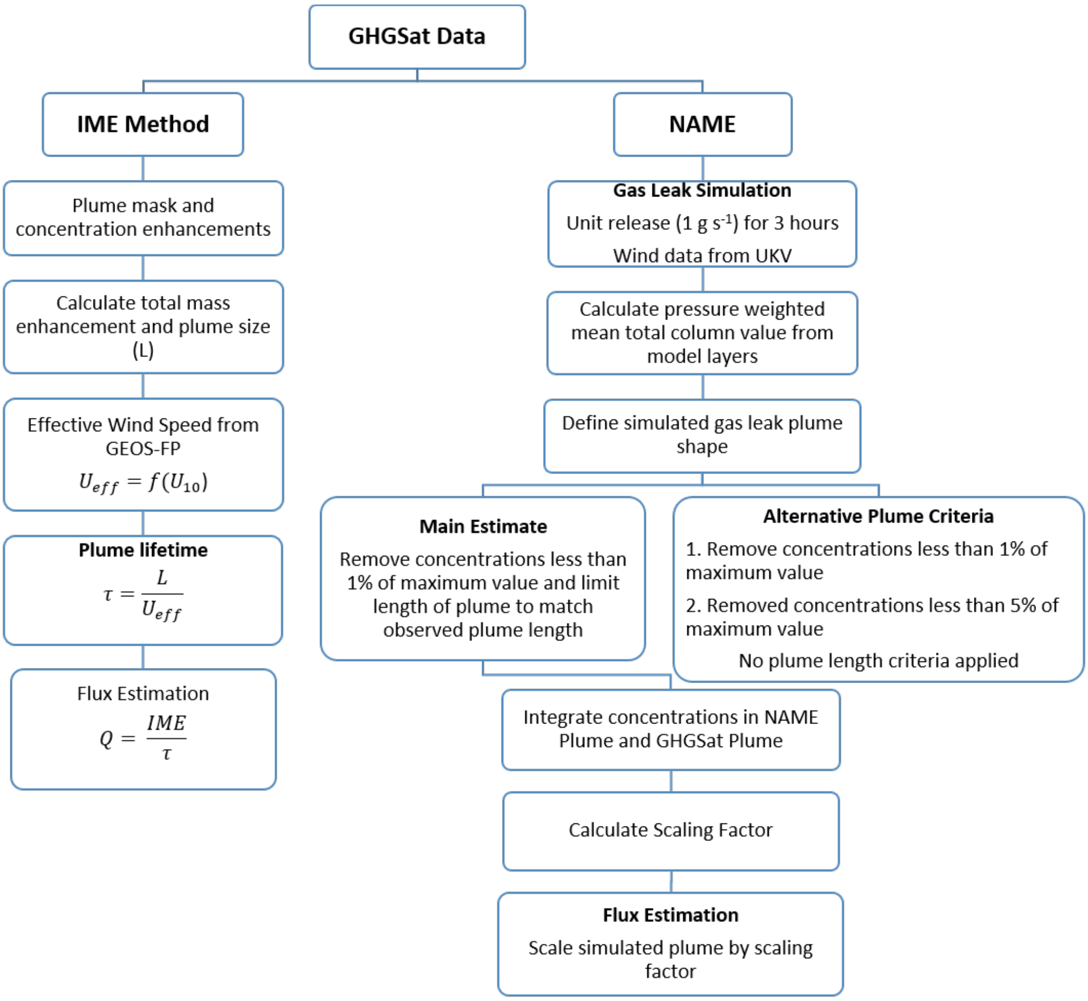

Figure S4. Flow-chart showing flux estimation methods using GHGSat data. The IME Method flow-chart has been adapted from Varon et al. (2018).

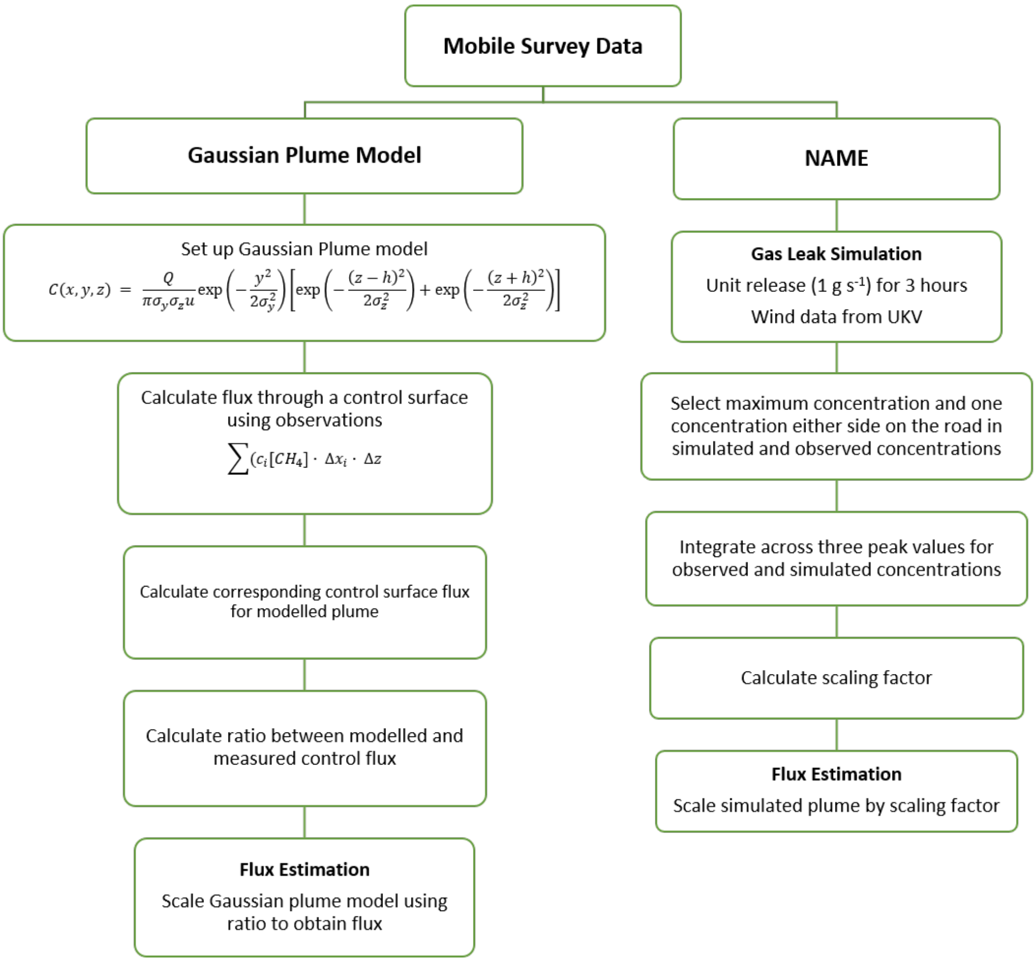

Figure S5. Flow-chart showing flux estimation methods using mobile survey observations.

Section S4. Mobile Survey

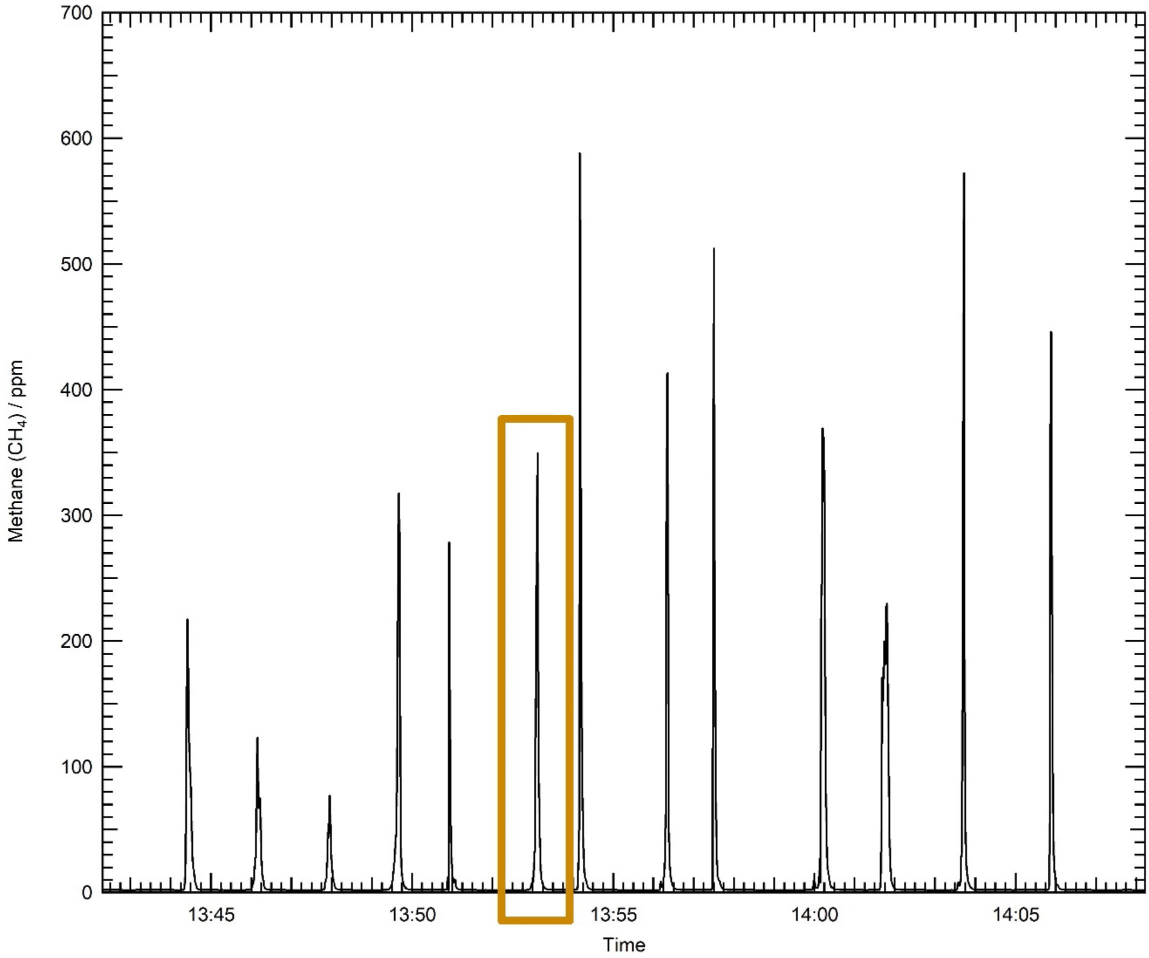

Figure S6. CH_4 concentrations observed during the 26th May mobile survey transects. The median plume is highlighted by the orange box.

The time-series of CH_4 mixing ratio data from the May mobile-survey can be found in the Figure S6. It shows 13 transects, with the median plume displayed in Figure S6 shown with the orange outline.

The variability in the plume expected to be driven by a combination of meteorology and inconsistent flux rates. This inherent variability in measurements made during mobile transect measurements can be seen in other studies of this nature, such as Caulton et al., (2018). Averaging of the fluxes derived from each individual transect has been demonstrated to be an effective method to estimate a true flux under controlled release conditions to within approximately 40% (Kumar et al., 2021).

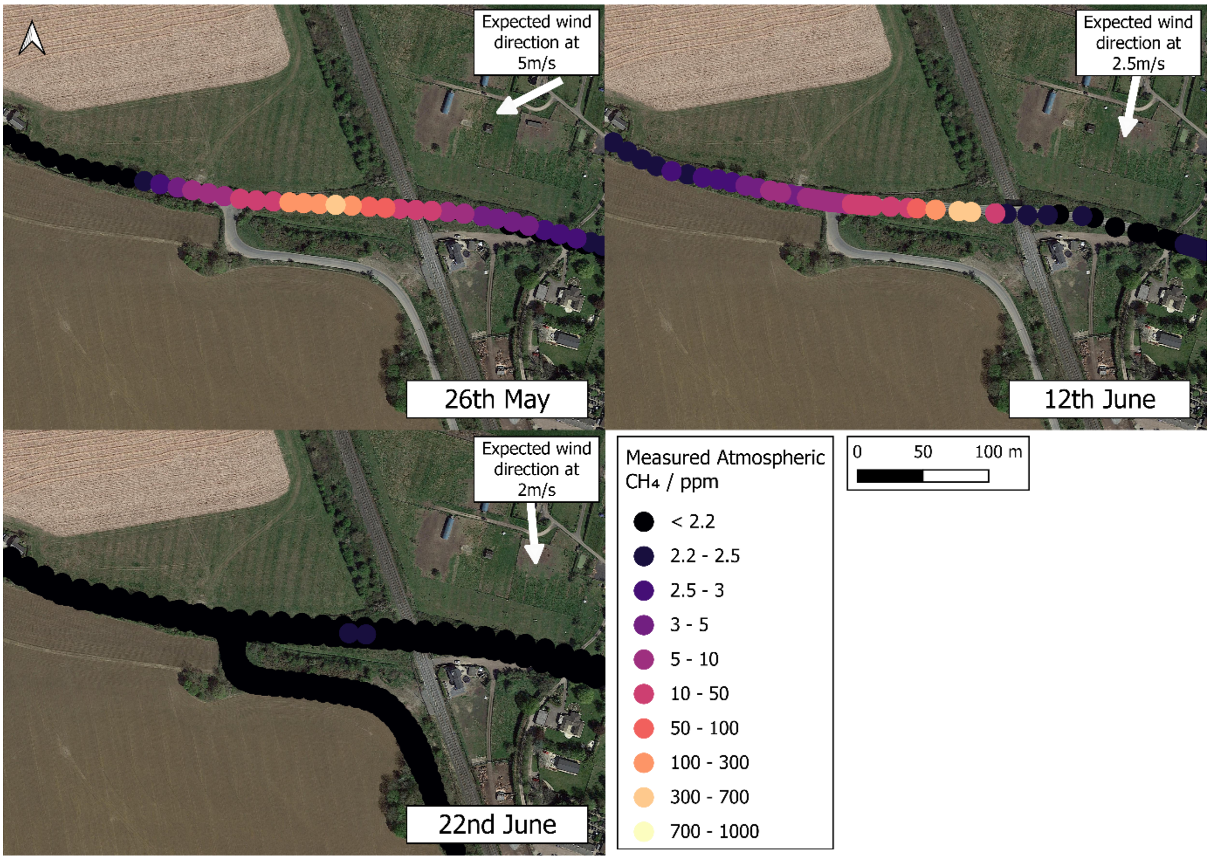

Figure S7. Median observed concentrations (ppb) during the ground-based mobile surveys. © Google Maps 2023

Table S2 Atmospheric stability classification based on wind speed (m s^{-1}) and sky conditions.

	Daytime insolation			**Night-time conditions**	
Surface wind speed (m s^{-1})	**Strong**	**Moderate**	**Slight**	**Thin overcast or > 4/8 low cloud**	**<= 4/8 cloudiness**
< 2	A	A - B	B	E	F
2-3	A - B	B	C	E	F
3-5	B	B - C	C	D	E
5-6	C	C - D	D	D	D
> 6	C	D	D	D	D

Section S5. NAME Plume Modelling

We tested different plume criteria for scaling NAME to estimate the flux of the leak from the satellite. Here are the different flux estimates from the different plume criteria.

Table S3. Comparison between the mobile survey- and GHGSat-derived fluxes (kg h^{-1}) against the equivalent fluxes derived in NAME (kg h^{-1}) with the release location moved by ~10m in N/S/E/W directions. The NAME-derived fluxes are shown with the estimation bounds in brackets.

Date	GHGSat Flux (kg h^{-1})	Mobile Survey Flux (kg h^{-1})	NAME Derived Flux (kg h^{-1})	NAME Flux North (kg h^{-1})	NAME Flux South (kg h^{-1})	NAME Flux East (kg h^{-1})	NAME Flux West (kg h^{-1})
27/03/2023	236 ± 157	-	181 [135, 329]	199 [132,294]	206 [132,296]	202 [134,314]	208 [132,290]
20/04/2023	1071 ± 310	-	745 [539, 1376]	732 [560,1808]	769 [559,1813]	724 [559,1782]	776 [560,1868]
20/05/2023	1375 ± 481	-	1243 [931, 2322]	1462 [977,3128]	1498 [973,3128]	1455 [971,3018]	1444 [979,3123]
26/05/2023	-	846 ± 453	406 [366,680]	699 [513,920]	565 [505,860]	402 [369,578]	574 [510,823]
22/05/2023	438 ± 215	-	408 [169, 286]	398 [177,395]	432 [177, 397]	392 [177,396]	432 [177,403]
07/06/2023	290 ± 131	-	204 [77, 241]	212 [77,231]	210 [76,226]	211 [75,208]	229 [76,228]
12/06/2023	-	634 ± 299	512 [498,681]	812 [785,1147]	729 [701,990]	511 [502,671]	794 [750,1130]

Table S4. Wind speeds (ms^{-1}) used in flux estimations.

Date	GEOS FP Wind Speed (ms^{-1})	GEOS-FP Wind Direction (°)	UKV Wind Speed (ms^{-1})	UKV Wind Direction
27/03/2023	0.8	119 (ESE)	3.8	163 (SSE)
20/04/2023	7.3	45 (NE)	12.0	46 (NE)
20/05/2023	4.9	40 (NE)	7.3	44 (NE)
22/05/2023	5.3	6 (N)	8.6	13 (N)
26/05/2023	-	-	4.4	79 (ENE)
07/06/2023	3.7	66 (ENE)	5.8	76 (ENE)
12/06/2023	-	-	3.1	46 (NE)

Section S6. Modelled Concentrations at Ridge Hill

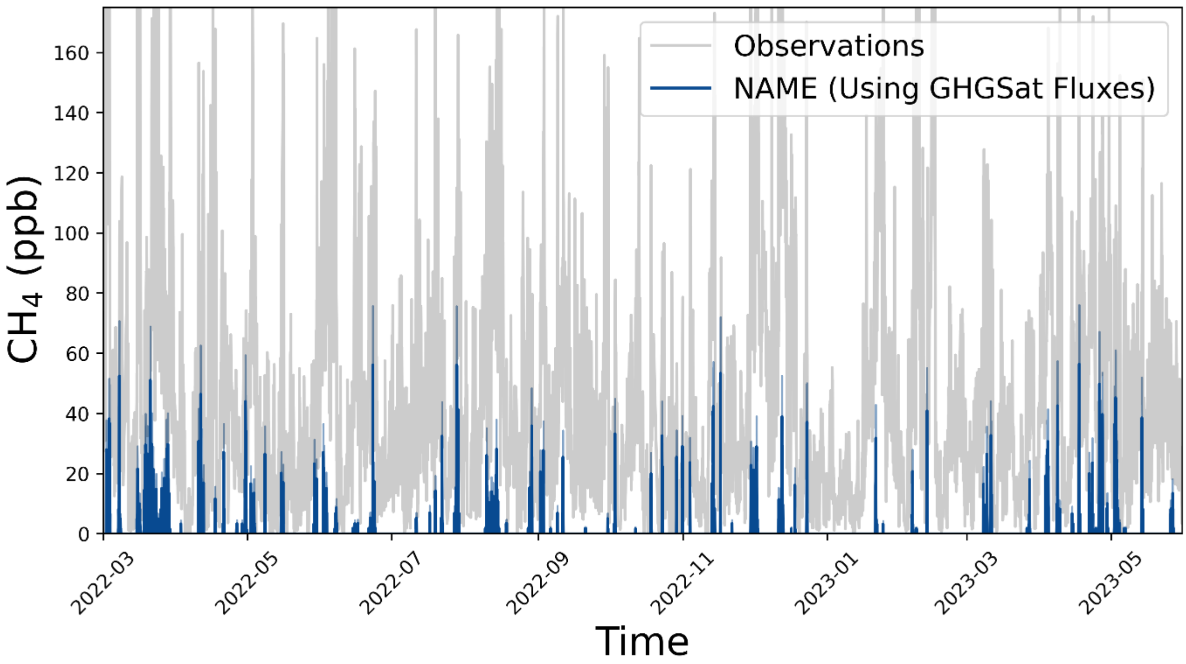

Figure S8. The NAME_long modelled concentrations at Ridge Hill from GHGSat derived flux rates (ppb, blue) and above-background concentrations at RGL (ppb, grey).

References

Caulton, D. R., Li, Q., Bou-Zeid, E., Fitts, J. P., Golston, L. M., Pan, D., Lu, J., Lane, H. M., Buchholz, B., Guo, X., McSpiritt, J., Wendt, L., and Zondlo, M. A.: Quantifying uncertainties from mobile-laboratory-derived emissions of well pads using inverse Gaussian methods, Atmospheric Chemistry and Physics, 18, 15145–15168, https://doi.org/10.5194/acp-18-15145-2018, 2018.

Kumar, P., Broquet, G., Yver-Kwok, C., Laurent, O., Gichuki, S., Caldow, C., Cropley, F., Lauvaux, T., Ramonet, M., Berthe, G., Martin, F., Duclaux, O., Juery, C., Bouchet, C., and Ciais, P.: Mobile atmospheric measurements and local-scale inverse estimation of the location and rates of brief CH_4 and CO_2 releases from point sources, Atmospheric Measurement Techniques, 14, 5987–6003, https://doi.org/10.5194/amt-14-5987-2021, 2021.